The FASEB Journal article fj.11-202317. Published online July 20, 2012.

Srgap3$^{-/-}$ mice present a neurodevelopmental disorder with schizophrenia-related intermediate phenotypes

Robert Waltereit,[*,†] Uwe Leimer,[*] Oliver von Bohlen und Halbach,[‖] Jutta Panke,[*] Sabine M. Hölter,[¶] Lillian Garrett,[¶] Karola Wittig,[§] Miriam Schneider,[‡] Camie Schmitt,[*] Julia Calzada-Wack,[#] Frauke Neff,[#] Lore Becker,[,††] Cornelia Prehn,[**] Sergej Kutscherjawy,[*] Volker Endris,[‡‡] Claire Bacon,[‡‡] Helmut Fuchs,[**] Valérie Gailus-Durner,[**] Stefan Berger,[*] Kai Schönig,[*] Jerzy Adamski,[**] Thomas Klopstock,[††] Irene Esposito,[#,§§] Wolfgang Wurst,[‖‖,¶¶,##] Martin Hrabě de Angelis,[**,***] Gudrun Rappold,[‡‡] Thomas Wieland,[§] and Dusan Bartsch[*,1]**

[*]Department of Molecular Biology, [†]Department of Psychiatry, and [‡]Institute of Psychopharmacology, Central Institute of Mental Health and Heidelberg University, and [§]Institute of Experimental and Clinical Pharmacology and Toxicology, Heidelberg University, Medical Faculty Mannheim, Mannheim, Germany; [‖]Institute of Anatomy and Cell Biology, University of Greifswald, Greifswald, Germany; [¶]Institute of Developmental Genetics, [#]Institute of Pathology, and **German Mouse Clinic, Institute of Experimental Genetics, Helmholtz Zentrum München, Neuherberg, Germany; [††]Department of Neurology, Friedrich-Baur-Institute, Ludwig-Maximilians-Universität München, Munich, Germany; [‡‡]Department of Molecular Human Genetics, University of Heidelberg, Heidelberg, Germany; [§§]Institut für Allgemeine Pathologie und Pathologische Anatomie der Technischen Universität München, Munich, Germany; [‖‖]Max Planck Institute of Psychiatry, Munich, Germany; [¶¶]Deutsches Zentrum für Neurodegenerative Erkrankungen, Munich, Germany; and [##]Lehrstuhl für Entwicklungsgenetik and ***Lehrstuhl für Experimentelle Genetik, Technischen Universität München, Freising-Weihenstephan, Germany

ABSTRACT **Mutations in the *SRGAP3* gene residing on chromosome 3p25 have previously been associated with intellectual disability. Genome-wide association studies have also revealed *SRGAP3*, together with genes from the same cellular network, as risk genes for schizophrenia. SRGAP3 regulates cytoskeletal dynamics through the RHO protein RAC1. RHO proteins are known to be involved in cytoskeletal reorganization during brain development to control processes such as synaptic plasticity. To elucidate the importance of *SRGAP3* in brain development, we generated *Srgap3*-knockout mice. Ten percent of these mice developed a hydrocephalus and died before adulthood. Surviving mice showed various neuroanatomical changes, including enlarged lateral ventricles, white matter tracts, and dendritic spines together with molecular changes, including an increased basal activity of RAC1. *Srgap3*$^{-/-}$ mice additionally exhibited a complex behavioral phenotype. Behavioral studies revealed an impaired spontaneous alternation and social behavior, while long-term memory was unchanged. The animals also had tics. Lower locomotor activity was observed in male *Srgap3*$^{-/-}$ only. *Srgap3*$^{-/-}$ mice showed increased methylphenidate stimulation in males and an impaired prepulse inhibition in females. Together, the results show neurodevelopmental aberration in *Srgap3*$^{-/-}$ mice, with many of the observed phenotypes matching several schizophrenia-related intermediate phenotypes. Mutations of *SRGAP3* may thus contribute to various neurodevelopmental disorders. Waltereit, R., Leimer, U., von Bohlen und Halbach, O., Panke, J., Hölter, S. M., Garrett, L., Wittig, K., Schneider, M., Schmitt, C., Calzada-Wack, J., Neff, F., Becker, L., Prehn, C., Kutscherjawy, S., Endris, V., Bacon, C., Fuchs, H., Gailus-Durner, V., Berger, S., Schönig, K., Adamski, J., Klopstock, T., Esposito, I., Wurst, W., Hrabě de Angelis, M., Rappold, G., Wieland, T., Bartsch, D. *Srgap3*$^{-/-}$ mice present a neurodevelopmental disorder with schizophrenia-related intermediate phenotypes. *FASEB J.* **26, 000–000 (2012). www.fasebj.org**

Key Words: intellectual disability · hydrocephalus · knockout mouse · RHO proteins · polygenetic disease

Abbreviations: CA1, cornu ammonis area 1; CDC42, cell division control protein 42 homolog; CNV, copy number variation; CYFIP1, cytoplasmic FMR1-interacting protein 1; DISC1, disrupted in schizophrenia 1; E, embryonic day; ERK1/2, extracellular signal-regulated kinase 1/2; GAP, GTPase-activating protein; IQ, intelligence quotient; MEGAP, mental disorder-associated GTPase-activating protein; PAK1, p21 protein (Cdc42/Rac)-activated kinase 1; PDGF, platelet-derived growth factor; PPI, prepulse inhibition; RAC1, Ras-related C3 botulinum toxin substrate 1; RHOA, Ras homolog gene family, member A; SHIRPA, SmithKline Beecham, Harwell, Imperial College, and Royal London Hospital phenotype assessment; SRGAP3, SLIT-ROBO RHO GTPase-activating protein 3

Rho GTPase PROTEINS play essential roles in the development and plasticity of the nervous system. Ras homolog gene family, member A (RHOA), Ras-related C3 botulinum toxin substrate 1 (RAC1), and cell division control protein 42 homolog (CDC42) regulate actin dynamics during neuronal development to control neuronal migration, axonal growth, and dendritic branching (1, 2). In mature neurons, they are involved in structural changes of dendritic spines during synaptic plasticity (3–7). RHO GTPases cycle between an active GTP-bound state and an inactive GDP-bound state. Dysfunction of RHO GTPases has been associated with several psychiatric and neurological diseases (1, 6). Of those, intellectual disability (previously called mental retardation) seems to be the most prominent clinical manifestation of aberrant RHO signaling (8–13).

The $3p^-$ syndrome is caused by deletions affecting many genes at the terminal end of chromosome 3p and is characterized by intellectual disability, microcephalus, muscle hypotonia, growth failure, heart and renal defects, and facial abnormalities (14). Our study began with the discovery of a balanced translocation, with one breakpoint mapping within the chromosomal 3p25 interval, in a female patient exhibiting "severe mental retardation," muscle hypotonia, and facial abnormalities. The translocation breakpoint was between exons 3 and 4 of the *SRGAP3* gene, which encodes SLIT-ROBO RHO GTPase-activating protein 3 (SRGAP3), also termed mental disorder-associated GTPase-activating protein (MEGAP). SRGAP3 is highly expressed in fetal and adult brain, including the cortex and the hippocampus (15, 16). *In vitro* it strongly activates intrinsic RAC1-GTPase activity and, to a lesser extent, CDC42 (17–19). The "severe mental retardation" used to describe the psychopathology of this patient was not defined by intelligence quotient (IQ) testing. Instead, the term relates here to a clinical diagnosis of severe psychomotoric retardation, attention deficits, and absence of speech (17). In an independent study, another patient was described with a mutation in exon 8 of the *SRGAP3* gene that led to the expression of a truncated SRGAP3 protein, and this patient had normal intelligence (20). Therefore, it is not clear whether loss of SRGAP3 function is causative for the cognitive impairment seen in patients with $3p^-$ syndrome.

Recent genome-wide association studies have revealed a significant overlap in the genes that lead to intellectual disability, autism, and schizophrenia, with a focus on shared trajectories in neurodevelopmental processes and synaptic plasticity (21–25). As individual genes can contribute to multiple neurodevelopmental disorders, *SRGAP3* may not be restricted to intellectual disability alone. A rank-based genome scan meta-analysis revealed rank three for the region 3p25.3-p22.1 for schizophrenia (26). Childhood-onset schizophrenia (COS) is a rare and severe form of schizophrenia with some similarities to autism. Within a sample of 105 patients with COS, rare copy number variations (CNVs) in *SRGAP3* were identified among a few other genes (27). Sixty-six *de novo* CNVs were identified in 1433 individuals with schizophrenia, and one of the affected genes encoded for cytoplasmic FMR1-interacting protein 1 (CYFIP1), which interacts with RAC1 (28). In addition, the schizophrenia risk factor disrupted in schizophrenia 1 (DISC1) regulates glutamatergic synapse formation *via* RAC1 (29).

To investigate the possibility that disruption of the *SRGAP3* gene causes neurodevelopmental disorders, we assessed the neuroanatomical and behavioral phenotype of *Srgap3*-deficient mice, which mimicked the translocation breakpoint described in the patient (17). *Srgap3*-deficient animals were also assessed in a systemic primary phenotypic screen at the German Mouse Clinic (30). The full data set from this screen is available at the Europhenome website (http://www.europhenome.org).

MATERIALS AND METHODS

Generation of knockout mice

The genomic mouse PAC clone RPCIP711J22374Q2 (Library RPCI-21; RZPD, Berlin, Germany) was used as a template to amplify the 3′ end of *Srgap3* exon 3 by PCR using the oligonucleotide sequences 5′-ATAAGAATGCGGCCGCAGCCCAGGGGACTCTCAGG-3′ and 5′-GCACCTCGAGTTATTACTTTTTGAAGAGTCTGATGACATCTTC-3′, at the same time introducing a stop-codon. The final targeting construct consisted of the mutated sequence and an additional 5-kb homology region upstream of *Srgap3* exon 3 and a 2-kb homology region downstream. Using standard methods, targeted R1 embryonic stem cells (31) were injected into murine blastocysts and implanted into pseudopregnant recipients. Chimeric mice were crossed with C57BL/6J mice. To remove the FRT-flanked Neo resistance cassette, mice were crossed with FLP-deleter mice [Tg(ACTFLPe)9205Dym/J]. The resulting *Srgap3*-knockout mice were backcrossed with C57BL/6J mice for 6 to 8 generations.

Animals

Mice were housed under a 12-h reversed day-night cycle. All testing took place during the night phase. Wild-type and $Srgap3^{-/-}$ genotypes were determined by PCR. Primers specific to the wild-type allele were 5′-TCAACGACATCTTCATGAAC-3′ and 5′-AAAGAGACCCAGGGCAGATA-3′, resulting in a 108-bp PCR product. Primers specific to the mutated $Srgap3^{-/-}$ allele were 5′-CCCTTAATTAACCGGTGAAG-3′ and 5′-AAAGGTTTTTATTCCTGTGG-3′, resulting in a 200-bp PCR product. PCR conditions were 94°C for 30 s, 56°C for 1 min, and 72°C for 1 min for 35 cycles. In all experiments, littermates with similar distribution to $Srgap3^{-/-}$ and wild-type and similar age were used. If not stated otherwise, animals were ≥12 but ≤40 wk old. All experimental procedures were performed according to permission obtained from local state authorities.

[1] Correspondence: Department of Molecular Biology, Central Institute of Mental Health, University of Heidelberg, J 5, 68159 Mannheim, Germany. E-mail: dusan.bartsch@zi-mannheim.de

doi: 10.1096/fj.11-202317

This article includes supplemental data. Please visit *http://www.fasebj.org* to obtain this information.

Pathology and histopathology

Gross and histological analyses were performed at the age of 17–20 wk (*Srgap3*$^{-/-}$: males n=8, females n=8; wild-type littermates: males n=8, females n=8). Animals were analyzed macroscopically (see http://eulep.pdn.cam.ac.uk/necropsy_of_the_mouse/index.php). The weights of the heart, spleen, and liver were determined. All organs were fixed in 4% buffered formalin, embedded in paraffin, and cut and stained with hematoxylin and eosin for histological evaluation. Sections were independently reviewed and interpreted by a neuropathologist (F.N.) and a medical scientist experienced in mouse pathology (J.C.-W.).

Analysis of fiber tracts

Serial coronal brain sections (30 μm thick), derived from *Srgap3*$^{-/-}$ (n=4) and wild-type (n=4) mice, were made using a vibratome (Leica VT1000; Leica Microsystems, Wetzlar, Germany). Sections were stained using the BrainStain Imaging kit (Molecular Probes, Eugene, OR, USA), according to the supplier's protocol. Stained sections were mounted in fluorescent mounting medium (Dako, Carpinteria, CA, USA). Regions of interest from one focal plane were captured by an Axiocam video camera (Zeiss, Oberkochen, Germany) mounted on an Axioplan 2 imaging microscope (Zeiss), under the control of the Axiovision 3.1 software (Zeiss). The mean thickness was analyzed using ImageTool 3.0 (University of Texas Health Science Center at San Antonio, San Antonio, TX, USA). Statistical analysis (unpaired t test) was performed using Prism 5.03 (Graph Pad, San Diego, CA, USA).

Golgi-Cox staining and dendritic spine analysis

Brains were impregnated according to the Golgi-Cox procedure (32) using Rapid GolgiStain reagents (FD NeuroTechnologies, Columbia, MD, USA) and cut at 100 μm. Analysis of dendritic spines was conducted in a blinded procedure. Only tertiary dendrites were evaluated, which displayed no breaks in their staining and were not obscured by other neurons or artifacts. Only one segment per individual dendritic branch and neuron was chosen for the analysis. Three-dimensional reconstruction and evaluation were performed using NeuroLucida (Microbrightfields, Williston, VT, USA), as described previously (33). The N values for the statistical analysis (unpaired t test) were based on animal numbers (N) and not on numbers of analyzed elements (n). Sampling was optimized to produce a coefficient of error (CE) under the observed biological variance (34). Spines were grouped into very short (≤0.5 μm), short (>0.5 to ≤1 μm), medium (>1 to ≤1.5 μm), long (>1.5 to ≤2 μm) and very long (>2 μm) spines. Data were analyzed (2-way ANOVA followed by Bonferroni *post hoc* test) using Prism 5.03 (Graph Pad).

Clinical chemistry, energy metabolism, and steroid metabolism

These parameters were determined as described previously (35). Clinical chemistry consisted of white blood cell (WBC), red blood cell (RBC), platelet, hemoglobin, hematocrit, mean corpuscular volume (MCV), mean corpuscular hemoglobin (MCH), calcium, albumin, transferrin, cholesterol, triglyceride, and glucose assays. Energy metabolism assessed body weight, rectal body temperature, food intake, mean oxygen consumption, mean respiratory quotient, and minimal oxygen consumption. Steroid metabolism comprised dehydroepiandrosterone (DHEA) and testosterone.

Quantitative Western blot analysis

Whole cortices were frozen in liquid nitrogen, sonicated in protein lysis buffer, and immunoblotted (36). Blots were hybridized with mouse monoclonal anti-phospho-p44/42-MAPK (1:2000) and rehybridized after stripping with rabbit polyclonal anti-p44/42-MAPK (1:1000) antibodies (Cell Signaling Technology, Beverly, MA, USA). The polyclonal antibody against SRGAP3 was raised in rabbit using synthetic peptides (NH_2-CHELRELERQNTVKQ-$CONH_2$). The antibody was purified over a SRGAP3-conjugated Sepharose 4B column (Pineda Antibody Service, Berlin, Germany). Signals on autoradiographs were quantified with a densitometer.

RAC1 activity

Mouse embryonic fibroblasts (MEFs) were isolated and cultured according to standard protocols (37). Wild-type and *Srgap3*$^{-/-}$ embryos were harvested at embryonic day (E) 13.5, and a cell suspension was prepared from the embryonic tissue. MEFs were cultured in DMEM (Invitrogen, Carlsbad, CA, USA) supplemented with 10% FBS. The cellular level of GTP-loaded RAC1 was determined essentially as described previously (38, 39). In brief, MEFs from wild-type and *Srgap3*$^{-/-}$ mice were grown to confluency in 6-cm dishes, serum starved for 24 h, and then treated with 50 ng/ml platelet-derived growth factor (PDGF; Sigma-Aldrich, St. Louis, MO, USA) for 1 min at 37°C. Thereafter, the cells were lysed, and the RAC1-containing supernatant was then incubated for 1 h at 4°C with a GST fusion protein containing the binding domain of p21 protein (Cdc42/Rac)-activated kinase 1 (PAK1) bound to magnetic glutathione Sepharose beads. The beads were washed and separated by SDS-PAGE. Rac1 was detected by immunoblotting with anti-RAC1 antibody (BD Transduction Laboratories, Lexington, KY, USA).

Neurological examination

Standardized neurological analysis of transgenic mice has been described previously (35, 40). Systematic observation was performed, according to a modified SmithKline Beecham, Harwell, Imperial College, and Royal London Hospital phenotype assessment (SHIRPA) protocol (41) for the assessment of basic neurological functions. Grip strength was analyzed by measuring the force a mouse applies to a grid attached to a force meter. Coordination and balance were determined with an accelerating rotarod (4 to 40 rpm in 5 min) in 3 trials with 15-min intertrial intervals.

Behavioral tests

Open-field and methylphenidate challenge

Eight chambers of equal size (48×48×40 cm) had dark floors and transparent walls. The chambers were surrounded with photobeam sensor rings, at 1 and 6 cm above the floor, which detected all movements (TruScan, Coulbourn Instruments, Allentown, GA, USA). Locomotor activity was monitored for 150 min, and signals were analyzed using TruScan software. After 30 min in the arena, mice received an intraperitoneal injection with 7.5 mg/kg methylphenidate (dissolved in PBS; Sigma-Aldrich) or vehicle control.

Y maze

The apparatus had an arm length of 32.5 cm, an arm width of 8.5 cm, and a height of 15 cm. It was made from light gray

PVC. Arms were covered with Plexiglas. The room was illuminated at 30 lux. The mouse was placed in the middle of the maze, and the experimenter left the room. Movements were recorded with a digital video camera for 5 min and analyzed manually by a trained observer. Entries into arms, including the whole body, were analyzed for their alternating behavior as blocks of 3 entries.

Prepulse inhibition (PPI)

PPI of the acoustic startle reflex (ASR) was assessed using a startle apparatus setup (Med Associates, St. Albans, VT, USA), including 4 identical sound-attenuating cubicles. The protocol used was based on the Eumorphia protocol (see http://www.empress.har.mrc.ac.uk), adapted to the specifications of our startle equipment, as described previously (42). Background noise (NS, no stimulus) was 65 dB, and trial types for ASR included 7 different stimulus intensities (NS, 70, 80, 90, 100, 110, 120 dB). Trial types for PPI included 4 different prepulse intensities (67, 69, 73, 81 dB); each prepulse preceding the startle pulse (110 dB) by a 50-ms interstimulus interval.

Social interaction

Social interaction was assessed in the open field (43). Animals were allowed to explore the test arena freely for 2 min before the social partner (male juvenile mouse, 6 wk old) was presented for 5 min. Behavior was videotaped, and the following elements were quantified by a trained observer in a blinded procedure: social behavior [contact behavior (grooming, crawling over), social exploration (anogenital and nonanogenital investigation), and approach and following], social avoidance/anxiety-related behavior (evasion on social contact and occurrence of stretched-attend posture), and self-grooming behavior.

Statistics

If not stated otherwise, graphs show means ± SE and significant results from 2-way ANOVA. Significant results from Bonferroni *post hoc* tests are indicated in the graphs as well. Differences were considered statistically significant at values of $P < 0.05$.

RESULTS

Generation of *Srgap3*$^{-/-}$ mice

We generated mice carrying a stop codon at the end of the 163-bp exon 3 of *Srgap3* by gene targeting (**Fig. 1*A***). The mutation resembled the breakpoint of the *t*(3; X)(p25;p11) translocation reported by Endris *et al.* (17). SRGAP3 is normally expressed in adult cortex of wild-type mice (15–17). We were able to show an apparent loss of SRGAP3 in the cortex of *Srgap3*$^{-/-}$ mice (Fig. 1*B, C*). By the knockout strategy applied, it could not be ruled out that a peptide comprising the first 141 of 1099 aa of SRGAP3 was still expressed, but because of strong homology with SRGAP1 and SRGAP2, there is no antibody available specific to the N terminus of Srgap3 to resolve this issue. *Srgap3*$^{-/-}$ mice are viable, and *Srgap3*$^{+/-}$ animals breed normally, according to the mendelian law, and littermates reach the same body weight. Clinical chemistry and energy metabolism in *Srgap3*$^{-/-}$ mice were normal, except for serum testosterone, which was lower in male *Srgap3*$^{-/-}$ animals (wild type, n=10, 0.908 ng/ml; *Srgap3*$^{-/-}$, n=8, 0.258 ng/ml; P=0.007).

Ten percent of *Srgap3*$^{-/-}$ mice die from hydrocephalus; most of the remaining animals have enlarged lateral ventricles

We performed a complete macroscopic and microscopic pathological assessment of mutant mice and wild-type controls. Approximately 10% of all *Srgap3*$^{-/-}$ mice developed a hydrocephalus and died at a median age of 50 d (**Fig. 2*A***). Hydrocephalus was not observed in any *Srgap3*$^{+/-}$ animals. *Srgap3*$^{-/-}$ mice without hydrocephalus reached the same age as wild-type and *Srgap3*$^{+/-}$ mice. The hydrocephalus was already apparent on macroscopical examination and necropsy (Fig. 2*Ca*) and was confirmed with microscopical examination (Figure 2*Cb*). Seventy-five percent of those *Srgap3*$^{-/-}$ mice without hydrocephalus presented enlarged lateral ventricles and periventricular edema on microscopical examination (Fig. 2*Bb, c* and Supplemental Fig. S1). No further gross

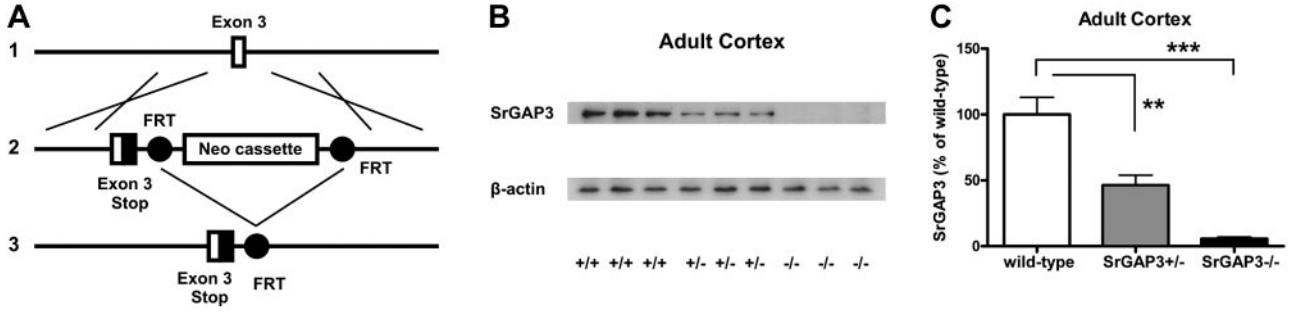

Figure 1. Generation of *Srgap3*$^{-/-}$ mice. *A*) Gene-targeting approach. *1*) *Srgap3* gene locus. *2*) Knockout gene locus after homologous recombination. *3*) *Srgap3*-null mutation following FLP-mediated recombination of FRT sites. *B, C*) Quantitative Western blot analysis of SRGAP3 expression in adult cortex. Females: wild type, n = 3; *Srgap3*$^{+/-}$, n = 3; *Srgap3*$^{-/-}$, n = 3. *B*) Autoradiographs. *C*) Signals quantified by densitometry. $^{**}P < 0.01$, $^{***}P < 0.001$; ANOVA with Bonferroni *post hoc* test. ANOVA.

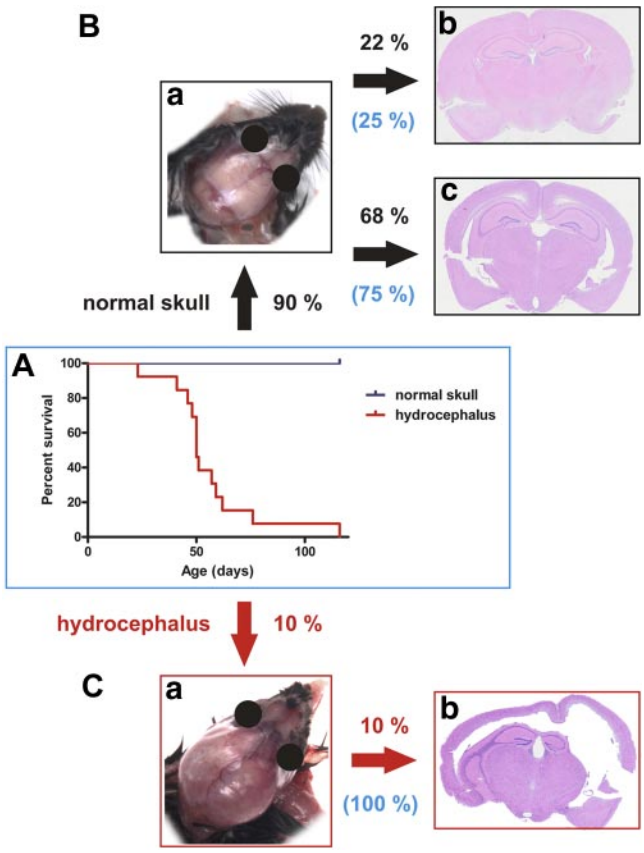

Figure 2. Ten percent of *Srgap3*$^{-/-}$ mice die from hydrocephalus. Most of the remaining animals have enlarged lateral ventricles. *A*) Survival of *Srgap3*$^{-/-}$ mice with hydrocephalus. Ten percent of all *Srgap3*$^{-/-}$ mice develop a macroscopically visible hydrocephalus. These animals died at a median age of 50 d (n=13). *B*) *a*) Ninety percent of *Srgap3*$^{-/-}$ mice have a macroscopically normal skull (n=16; eyes have been masked). *b*) Of *Srgap3*$^{-/-}$ mice with macroscopically normal skull, 25% have normal lateral ventricles on histopathological examination (n=4/16). Thus, 22% of all *Srgap3*$^{-/-}$ mice have normal lateral ventricles. *c*) Of *Srgap3*$^{-/-}$ mice with macroscopically normal skull, 75% have enlarged lateral ventricles on histopathological examination (n=12/16). Thus, 68% of all *Srgap3*$^{-/-}$ mice have enlarged lateral ventricles. *C*) *a*) Ten percent of *Srgap3*$^{-/-}$ mice have a macroscopically visible hydrocephalus (eyes have been masked). *b*) The hydrocephalus is always seen on histopathological examination, too. Thus, 10% of all *Srgap3*$^{-/-}$ mice have a hydrocephalus on histopathological examination.

morphological abnormalities were observed, including the testes. We only included those animals without hydrocephalus and with a minimum age of 12 wk in all following experiments.

Srgap3$^{-/-}$ mice have enlarged white matter tracts and longer dendritic spines

We next analyzed the neuroanatomy of *Srgap3*$^{-/-}$ mice. Brains were stained using the brain stain kit and assessed by fluorescence microscopy. White matter tracts were enlarged in *Srgap3*$^{-/-}$ brains (**Fig. 3*A***). This enlargement was most prominent in the corpus callosum, where fiber tracts were ~30% thicker compared to wild-type animals. We also found a 20% enlargement in alveus and external capsule (Fig. 3*B*). No additional major alterations in the gross anatomy of the gray matter were found. As disturbances in RHO-signaling cascades are often associated with alterations in dendritic spines (5–7), we analyzed the morphology of cornu ammonis area 1 (CA1) pyramidal neurons in the hippocampus of Golgi-Cox-impregnated brains (Fig. 3*C*, *D*). Dendritic trees showed normal branching, and spine densities in *Srgap3*$^{-/-}$ mice were indistinguishable from wild-type animals (Fig. 3*E*, *G*). However, in both basal and apical dendrites, spines were longer in *Srgap3*$^{-/-}$ brains than in wild type (Fig. 3*F*, *H*).

Srgap3$^{-/-}$ mice exhibit an increased basal RAC1 activity

In vitro experiments have shown that SRGAP3 is a RAC1 GAP (17, 19). Thus, lack of SRGAP3 may result in increased RAC1 activity. We isolated embryonic fibroblasts from wild-type and *Srgap3*$^{-/-}$ animals and stimulated the activation of RAC1-GTP with 50 ng/ml PDGF for 1 min. Fibroblasts from *Srgap3*$^{-/-}$ mice were unresponsive to PDGF stimulation (**Fig. 4*A*, *B***). As RAC1 induces a signal transduction cascade from PAK to extracellular signal-regulated kinase 1/2 (ERK1/2) *via* rapidly accelerated fibrosarcoma kinase (RAF) and MAPK/ERK kinase (MEK) (44), we analyzed the level of phosphorylated ERK1/2 in the adult cortex. As shown in Fig. 4*C*, the concentration of phosphorylated ERK2 was higher in *Srgap3*$^{-/-}$ mice compared to wild-type animals (Fig. 4*C*).

Srgap3$^{-/-}$ mice express lower locomotor activity, have tics, and are impaired in spontaneous alternation, while long-term memory is normal

We thoroughly investigated the behavioral phenotype of the *Srgap3*$^{-/-}$ mice using a series of tests. We used the open-field test to assess locomotor activity. Male *Srgap3*$^{-/-}$ mice were less active than wild-type mice (**Fig. 5*A***), but no difference was observed in female *Srgap3*$^{-/-}$ mice (Fig. 5*B*). To investigate whether *Srgap3*$^{-/-}$ mice have abnormal anxiety, we used the light/dark box and the elevated plus maze. Both tests revealed no differences between *Srgap3*$^{-/-}$ and wild-type animals (Supplemental Fig. S2). We then performed a full neurological examination according to the SHIRPA-protocol (41), which showed that *Srgap3*$^{-/-}$ mice have spontaneous tics (Fig. 5*C*). The remaining neurological examination was unremarkable, with no abnormalities in coordination and muscle strength. Analysis of memory function was performed using the Y maze, where spontaneous alternation is attributed to working memory. In *Srgap3*$^{-/-}$ mice, spontaneous alternation was reduced (Fig. 5*D*). Long-term memory in humans is often divided into procedural (implicit) and declarative (explicit) memory. Classical conditioning is attributed to procedural memory. We analyzed classical conditioning by fear conditioning (Supplemental Fig. S3) and by

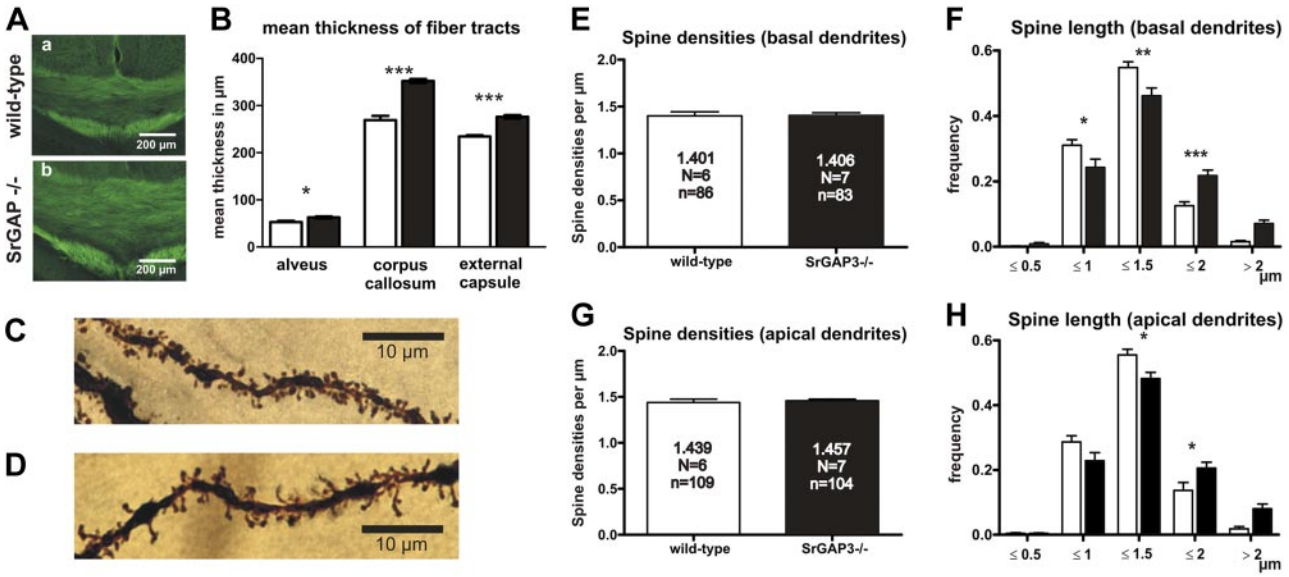

Figure 3. Srgap3$^{-/-}$ mice have enlarged white matter tracts and longer dendritic spines. *A*) Differences in the mean thickness of the corpus callosum are obvious by comparing FluroMyelin stainings of control (*a*) and *Srgap3*-deficient mice (*b*). *B*) The mean thickness of the alveus, corpus callosum, and external capsule was increased in the *Srgap3*-deficient mice as compared to their controls $*P \leq 0.05$, $***P \leq 0.001$; unpaired *t* test. *C*) Golgi-Cox staining of a hippocampal dendrite of a wild-type mouse. *D*) Golgi-Cox staining of a hippocampal dendrite of a *Srgap3*$^{-/-}$ mouse. *E*) No significant change (P=0.921; unpaired *t* test) in spine densities of basal dendrites of CA1 pyramidal neurons was found. *F*) Mean length of dendritic spines on basal dendrites of CA1 pyramidal neurons was altered; thus, a shift toward longer spines was noted in case of the *Srgap3*-knockout mice. $*P \leq 0.05$, $**P \leq 0.005$, $***P \leq 0.001$; 2-way ANOVA with Bonferroni *post hoc* test. *G*) Mean spine densities of apical dendrites of CA1 pyramidal neurons was unaltered (P=0.662; unpaired *t* test). *H*) Mean length of spines on apical dendrites of CA1 pyramidal neurons was altered. A shift toward longer spines was noted in case of the *Srgap3*-knockout mice. $*P \leq 0.05$, $**P \leq 0.005$, $***P \leq 0.001$; 2-way ANOVA with Bonferroni *post hoc* test.

conditioned taste aversion (Supplemental Fig. S4). *Srgap3*$^{-/-}$ mice generally showed longer freezing rates, which is in accordance with the reduced locomotor activity. For conditioned taste aversion, there were no differences between genotypes. We proceeded with long-term memory paradigms attributed to declarative memory. Spatial memory was assessed in the Morris water maze and was not impaired in *Srgap3*$^{-/-}$ animals (Supplemental Fig. S5). Finally, we studied object recognition memory and found no impairment in the short-term (15-min interval) or the long-term memory (24-h interval), although *Srgap3*$^{-/-}$ mice did spend less time exploring the objects (Supplemental Fig. S6).

Social behavior is impaired in *Srgap3*$^{-/-}$ mice

We have demonstrated some behavioral alterations in *Srgap3*$^{-/-}$ mice, but despite a reduction in spontaneous alternation, cognition appeared to be intact. These findings prompted us to investigate another major paradigm of behavior: social interaction. The interaction of *Srgap3*$^{-/-}$ and wild-type mice with an unknown social partner was analyzed. Social exploration was divided into anogenital, nonanogenital exploration, and approach and follow behavior. Anogenital exploration was reduced in both male and female *Srgap3*$^{-/-}$ animals (Fig. 5*E*). Nonanogenital exploration (Sup-

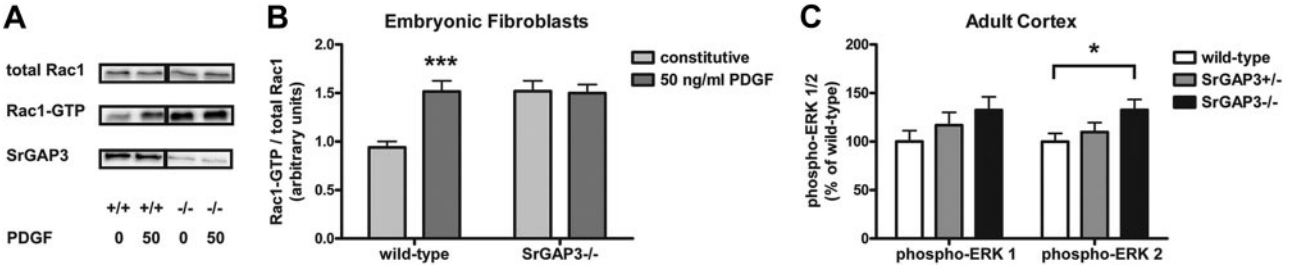

Figure 4. Srgap3$^{-/-}$ mice exhibit increased RAC1 activity. *A, B*) RAC1 activity in embryonic fibroblasts. Cells were analyzed for basal RAC1 activity and for activity 1 min after stimulation with 50 ng/ml PDGF. RAC1 activity was determined as relation of RAC1-GTP and total RAC1. *A*) Representative pulldown experiments. *B*) Quantification of RAC1-GTP activity as ratio of RAC1-GTP to total RAC1 content. Wild-type, $n = 6$; *Srgap3*$^{-/-}$, $n = 6$ (P>0.05 for basal *vs.* stimulated cells; ANOVA). $***P < 0.001$ *vs.* basal cells; ANOVA. *C*) ERK 1/2 activity in adult cortex. Phospho-ERK 1/2 and total ERK 1/2 were determined by quantitative Western blot analysis. Graph shows activity of phosphor-ERK 1/2 in relation to total ERK 1/2. Females: wild-type, $n = 9$; *Srgap3*$^{+/-}$, $n = 9$; *Srgap3*$^{-/-}$, $n = 9$. Phospho-ERK 1: $P > 0.05$ for *Srgap3*$^{+/-}$ and *Srgap3*$^{-/-}$ *vs.* wild type; ANOVA. Phospho-ERK 2: $P > 0.05$ for *Srgap3*$^{+/-}$ *vs.* wild type; ANOVA with Bonferroni *post hoc* test. $*P < 0.05$; ANOVA with Bonferroni *post hoc* test.

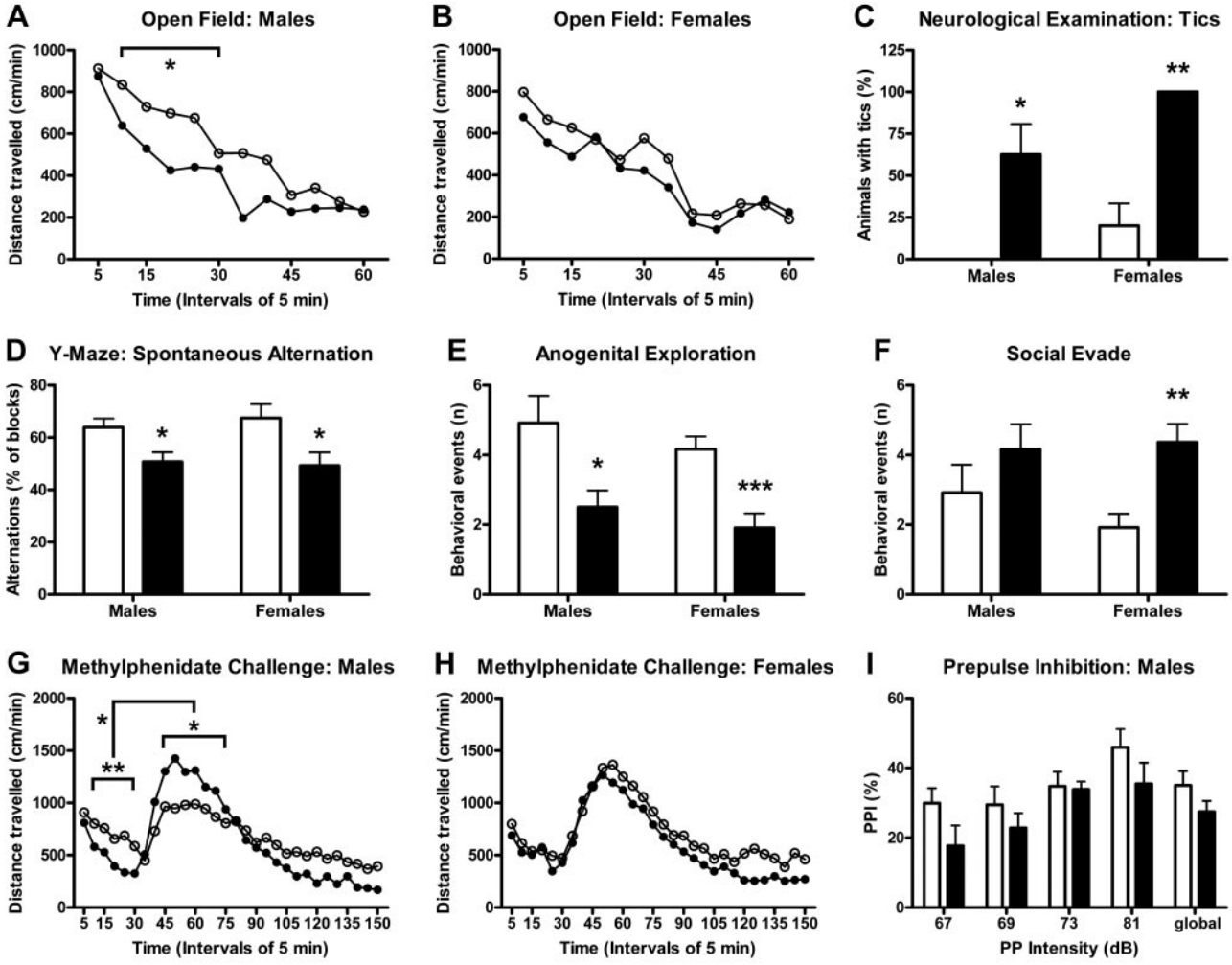

Figure 5. Srgap3$^{-/-}$ mice express lower locomotor activity, have tics, and are impaired in spontaneous alternation. Social behavior is impaired. Transgenic mice are sensitive to methylphenidate stimulation and impaired in PPI. *A*) Distance traveled in the open field. Males: wild-type, $n = 12$; *Srgap3*$^{-/-}$, $n = 12$. *$P < 0.05$ for intervals from 10 to 30 min; repeated-measures ANOVA. *B*) Distance traveled in the open field. Females: wild-type, $n = 11$; *Srgap3*$^{-/-}$, $n = 11$. $P > 0.05$ for intervals from 10 to 30 min; repeated-measures ANOVA. *C*) Tics in the SHIRPA protocol. Males: wild-type, $n = 10$; *Srgap3*$^{-/-}$, $n = 8$. Females: wild-type, $n = 10$; *Srgap3*$^{-/-}$, $n = 9$. *$P < 0.05$, **$P < 0.01$; ANOVA. *D*) Spontaneous alternation in the Y maze. Males: wild-type, $n = 12$; *Srgap3*$^{-/-}$, $n = 12$. Females: wild-type, $n = 12$; *Srgap3*$^{-/-}$, $n = 12$. *$P < 0.05$; ANOVA. *E*) Anogenital exploration. Males: wild-type, $n = 12$; *Srgap3*$^{-/-}$, $n = 12$. Females: wild-type, $n = 12$; *Srgap3*$^{-/-}$, $n = 11$. *$P < 0.05$, ***$P < 0.001$; ANOVA. *F*) Social evade. Males: wild-type, $n = 12$, *Srgap3*$^{-/-}$, $n = 12$; $P > 0.05$; ANOVA. Females: wild-type, $n = 12$; *Srgap3*$^{-/-}$, $n = 11$. **$P < 0.01$; ANOVA. *G*) Distance traveled in the open field. Intraperitoneal injection with 7.5 mg/kg methylphenidate after 30 min. Males: wild-type, $n = 10$; *Srgap3*$^{-/-}$, $n = 8$. *$P < 0.05$ for intervals from 45 to 75 min and for induction of intervals from 45 to 75 min from the intervals from 10 to 30 min, **$P < 0.01$ for intervals from 10 to 30 min; repeated-measures ANOVA. *H*) Distance traveled in the open field. Intraperitoneal injection with 7.5 mg/kg methylphenidate after 30 min. Females: wild-type, $n = 11$; *Srgap3*$^{-/-}$, $n = 11$; $P > 0.05$ for intervals from 10 to 30 min, intervals from 45 to 75 min, and for the induction of intervals from 45 to 75 min from the intervals from 10 to 30 min; repeated-measures ANOVA. *I*) PPI. Males: wild-type, $n = 10$; *Srgap3*$^{-/-}$, $n = 8$; $P > 0.05$ for all PPIs; ANOVA. *J*) PPI. Females: wild-type, $n = 10$; *Srgap3*$^{-/-}$ $n = 9$; $P > 0.05$ for 67, 69, 73 dB; ANOVA. *$P < 0.05$; ANOVA.

plemental Fig. S7*B*) and approach and follow behavior (Supplemental Fig. S7*C*) were reduced only in female *Srgap3*$^{-/-}$ mice. Contact behavior was not altered in *Srgap3*$^{-/-}$ animals (Supplemental Fig. S7*D*). Social evasion is the active avoidance of contact with the social partner and was increased in *Srgap3*$^{-/-}$ mice (Fig. 5*F*).

Srgap3$^{-/-}$ mice are sensitive to methylphenidate stimulation and impaired in PPI

Our analyses of *Srgap3*$^{-/-}$ mice revealed certain phenotypes, including enlarged lateral ventricles, thicker white matter tracts, impaired spontaneous alternation,

and impaired social behavior, all of which resemble schizophrenia-related intermediate phenotypes previously described in animal models of the disease. This prompted us to assess whether further schizophrenia-related intermediate phenotypes are present in *Srgap3*$^{-/-}$ mice. We assessed two further paradigms. Methylphenidate stimulates dopamine release in the striatum, which is increased in schizophrenia. Methylphenidate injection resulted in locomotor hyperactivation in all treated mice. This hyperactivation was stronger in male *Srgap3*$^{-/-}$ mice (Fig. 5*G*), but not in female *Srgap3*$^{-/-}$ animals (Fig. 5*H*). PPI is also known to be impaired in schizophrenia and is interpreted as a sensorimotor gating deficit. Acoustic startle response amplitudes were lower in both male and female *Srgap3*$^{-/-}$ mice but could still be easily measured (Supplemental Fig. S8). Male *Srgap3*$^{-/-}$ mice had a subtly impaired PPI (Fig. 5*I*), while female *Srgap3*$^{-/-}$ mice had a more pronounced and statistically significant impairment in PPI (Fig. 5*J*).

DISCUSSION

In this study, we have generated *Srgap3*$^{-/-}$ mice. Ten percent of these mice developed a hydrocephalus and died before adulthood. Surviving animals showed distinct neuroanatomical changes and an increased RAC1 basal activity. Several behavioral alterations were also observed in *Srgap3*$^{-/-}$ mice. These alterations included an impaired spontaneous alternation and social behavior, while long-term memory was unchanged. The animals also had tics. Lower locomotor activity was observed in male *Srgap3*$^{-/-}$ only. *Srgap3*$^{-/-}$ mice showed increased methylphenidate stimulation in males and an impaired prepulse inhibition in females. The range of phenotypes that we have identified are complex and raise the questions of how they are interrelated, how they can elucidate the cellular importance of SRGAP3 in neurodevelopmental processes, and how loss of SRGAP3 function can contribute toward neurodevelopmental disorders.

Congenital hydrocephalus is a medical condition in humans (45). It likely develops during neural stem cell proliferation and differentiation in the embryonic brain. About 40% of hydrocephalus cases have a genetic etiology. Most known genes involved in the formation of hydrocephalus are cytokines, growth factors, or related molecules in the cellular signaling pathways during early brain development (46). We observed a hydrocephalus in only 10% of *Srgap3*$^{-/-}$ mice, although 75% had enlarged lateral ventricles. This suggests a continuum of ventricle system pathology from lethal hydrocephalus in only a few cases, enlarged lateral ventricles in the majority and normal ventricles in the minority of *Srgap3*$^{-/-}$ animals. Interestingly, enlarged lateral ventricles are a characteristic finding in patients with schizophrenia (47) and have additionally been described in a series of other knockout animals with neurodevelopmental phenotypes. A number of these mice were also reported to be defective for schizophrenia-related genes, neuregulin 1 (*NRG1*; refs. 48, 49) and *DISC1* (50).

SRGAP3 is a GAP and negatively regulates RAC1. In *Srgap3*$^{-/-}$ mice, RAC1 activity was increased compared to wild-type mice, likely due to the loss of the inhibitory role of SRGAP3 on RAC1 activity. Interestingly, we observed an enlarged corpus callosum in *Srgap3*$^{-/-}$ mice, which contrasts to the agenesis of commissural axons reported in the corpus callosum of *Rac1*$^{-/-}$ mice (51, 52). These findings implicate RAC1 activity in corpus callosum formation, and our results suggest that SRGAP3 may control RAC1 activity in this process. We also found longer dendritic spines in hippocampal neurons of *Srgap3*$^{-/-}$ animals. In human disease, abnormalities in dendritic spine formation are observed in intellectual disability, autism, schizophrenia, and neurodegenerative disorders, including Alzheimer's disease (53–56). Evidence suggests that RAC1 contributes to the regulation of dendritic spine formation (57) and pathways activating RAC1, such as the EPHRIN B (EPHB)-receptor-KALIRIN pathway have been shown to influence dendritic spine morphogenesis (58). Recently, it was described that mice lacking the *Rac1 GAP* variants *Bcr* and *Abr* exhibit a higher basal RAC1 activity, which was associated with higher levels of phosphorylated ERK1/2 (59).

Behavioral studies revealed that *Srgap3*$^{-/-}$ mice have an intact long-term memory. The core symptom of intellectual disability in humans is an IQ < 70, which is usually strongly associated with a deficit in learning and memory. Most genetically defined animal models of intellectual disability syndromes demonstrate learning deficits (60). The phenotypes that we observed in the *Srgap3*$^{-/-}$ mice seem to correlate better with those seen in rodent models of schizophrenia rather than intellectual disability. The clinical schizophrenia phenotype comprises so-called positive, negative, and cognitive symptoms. Hypersensitivity to methylphenidate stimulation in animal models is seen as part of the modeling of positive symptoms and was attributed to hyperactivity in the subcortical dopamine system. Reduced locomotor activity and impaired social behavior are part of the modeling of negative symptoms. Impaired spontaneous alternation and impaired PPI can be attributed to the modeling of positive and cognitive symptoms in schizophrenia (61–64). In our study, we did not investigate whether these phenotypes could be altered by treatment with antipsychotic drugs. In contrast to the schizophrenia-related behaviors we observed in our *Srgap3*$^{-/-}$ model, tics are not seen as a symptom of schizophrenia. They are the core symptom of Tourette's syndrome and associated with dysfunction in the dopamine system. Similar to schizophrenia, medications regulating the dopamine system are used as a treatment for tics (65). Impairments in learning and memory are also frequently observed in schizophrenia mouse models; however we did not find any such deficits in our *Srgap3*$^{-/-}$ mice. Finally, many behavioral findings in *Srgap3*$^{-/-}$ mice show a sexual

dimorphism. Lower testosterone in male *Srgap3*$^{-/-}$ mice was not associated with morphological changes in testes. Although sexual dimorphism is not unusual in knockout mice, the underlying cause in *Srgap3*$^{-/-}$ animals remains unclear. An association between serum testosterone levels and the severity of negative symptoms in male patients with chronic schizophrenia has been described (66). Reduced locomotor activity in male *Srgap3*$^{-/-}$ mice could be caused by lower testosterone levels.

Recently, Soderling and colleagues (67) published another *Srgap3*$^{-/-}$ mouse model, termed WAVE-associated Rac GAP (*Wrp*)$^{-/-}$. In *Wrp*$^{-/-}$ mice, exon 3 is flanked by loxP-sites, constituting a conditional knockout. In *Wrp*$^{-/-}$ mice with hereditary deletion of exon 3, lateral ventricles are enlarged, and dendritic spines have reduced density in neuronal cultures. For behavioral testing, *Wrp*$^{-/-}$ animals were crossed with *Nestin-Cre*-positive mice, in which CRE (causes recombination)-recombinase activity is present in nervous tissue by E11. These mice have normal short-term memory, but impaired long-term memory, which led the researchers to conclude that the *Wrp*$^{-/-}$ mice model the *SRGAP3*-deficient intellectual disability described in the published case reports (17, 68). The behavioral phenotype reported in *Wrp*$^{-/-}$ mice differs from our findings in *Srgap3*$^{-/-}$ animals. Three main explanations may account for this discrepancy. First, exons 2 and 3 encode the inverse F-BAR (IF-BAR) domain, which is interrupted in *Wrp*$^{-/-}$ but intact in *Srgap3*$^{-/-}$ mice. The IF-BAR domain facilitates the lipid binding of SRGAP3, and it has been suggested to be required for normal intellectual abilities (67). However, the IF-BAR domain was left undisrupted in the translocation patient with psychomotoric retardation (17) and in the individual with normal intelligence with a mutation in exon 8 of the *SRGAP3* gene (20). Second, in the conditional-knockout *Wrp*$^{-/-}$ mice, SRGAP3 function is lost from E11 onwards, whereas in our *Srgap3*$^{-/-}$ mice, the mutation was constitutive. It is possible that the earlier loss of Srgap3 in our mice induces compensatory mechanisms resulting in a milder behavioral phenotype, including normal long-term memory. Finally, differences in the genetic backgrounds between *Srgap3*$^{-/-}$ and *Wrp*$^{-/-}$ mice could account for the divergent phenotypes. Differences in the genetic backgrounds of knockout mice generated at two different laboratories may be the result of strain differences in embryonic stem cells and in C57BL/6 mice used for backcrossing the founders.

In summary, we have described the neurodevelopmental phenotype of *Srgap3*$^{-/-}$ mice. The findings from *Srgap3*- and *Wrp*-knockout mice suggest that complex and fragile regulatory mechanisms exist within the SRGAP3 cellular network. Congenital hydrocephalus, schizophrenia-related, and intellectual disability-related behaviors are all associated with neurodevelopmental disorders. Several hundred genes are known to be causative for intellectual disability, autism and schizophrenia, with overlapping functions for many of the participating genes between the different clinical phenotypes (21–25). In polygenetically inherited neurodevelopmental disorders, these genes usually act by subtle dosage effects, caused by CNVs, and in the concerted action of many mutations. Homozygous deletion of such a gene could have a much stronger impact, with a phenotype specific to the individual gene function. We propose that *SRGAP3* is one of these genes. Subtle changes in the SRGAP3 cellular network could be causative for the spectrum of neuroanatomical and behavioral phenotypes. High penetrance of the *Srgap3* gene defect during early brain development could be the cause of hydrocephalus in a minority of animals. A lower penetrance of the defect may result in enlarged lateral ventricles, which are also seen in schizophrenia. Notably, hydrocephalus was not seen in *Srgap3*$^{+/-}$ mice. Constitutive loss of *SRGAP3* appears to lead to certain schizophrenia-related behaviors, whereas later disruption of the protein may lead to intellectual disability-related behaviors (55). Here, we studied knockout mice with homozygous deletion of *Srgap3*. Further functional analyses of animal models deficient for genes associated with neuronal development are required to elucidate the mechanisms of these genes in intellectual disability, schizophrenia, and other neurodevelopmental disorders. FJ

The authors thank Drs. Birgit Rathkolb and Eckhard Wolf for the clinical chemistry screening and Drs. Jan Rozman and Martin Klingenspor for the energy metabolism screening; Dr. Vera Baier and Stefano Clementi for help with initial experiments; Lena Wendler, Ariana Frömmig, Elke Hermann, Waltraut Stettinger, Albert Langer, Maria Kugler, Tamara Halex, Sabine Holthaus, Katrin Laube, Jacqueline Müller, Elenore Samson, Waldemar Schneider, and Lucie Thurmann for excellent technical support; and finally the Central Institute of Mental Health and German Mouse Clinic animal caretaker teams. The authors thank Dr. Beatrix Naton for excellent administrative support. The authors also thank the members of the German Mouse Clinic for comprehensive phenotyping of the *Srgap3*$^{-/-}$ mice and fruitful discussions. The work was supported by EU HEALTH-F2-2007-201714 DEVANX, Bundesministerium für Bildung und Forschung (BMBF) Bernstein Center for Computational Neuroscience Heidelberg/Mannheim grant 01GQ1003A and BMBF NGFN-Plus grant 01GS0851 to D.B.; Deutsche Forshungsgemeinschaft grant BO 1971/5-1 to O.V.B.U.H; BMBF NGFN-Plus grants 01GS0850 to S.M.H, L.G., J.C.-W., F.N., C.P., J.A., I.E., H.F., V.G.-D., W.W. and M.H.D.A. and 01GS0851 to L.B. and T.K.; and EU grant LSHG-2006-037188 to the German Mouse Clinic.

REFERENCES

1. Govek, E. E., Newey, S. E., and Van Aelst, L. (2005) The role of the Rho GTPases in neuronal development. *Genes Dev.* **19,** 1–49
2. Van Aelst, L., and Cline, H. T. (2004) Rho GTPases and activity-dependent dendrite development. *Curr. Opin. Neurobiol.* **14,** 297–304
3. Carlisle, H. J., and Kennedy, M. B. (2005) Spine architecture and synaptic plasticity. *Trends Neurosci.* **28,** 182–187
4. Fischer, M., Kaech, S., Knutti, D., and Matus, A. (1998) Rapid actin-based plasticity in dendritic spines. *Neuron* **20,** 847–854
5. Luo, L. (2000) Rho GTPases in neuronal morphogenesis. *Nat. Rev. Neurosci.* **1,** 173–180

6. Ramakers, G. J. (2000) Rho proteins and the cellular mechanisms of mental retardation. *Am. J. Med. Genet.* **94,** 367–371
7. Threadgill, R., Bobb, K., and Ghosh, A. (1997) Regulation of dendritic growth and remodeling by Rho, Rac, and Cdc42. *Neuron* **19,** 625–634
8. Allen, K. M., Gleeson, J. G., Bagrodia, S., Partington, M. W., MacMillan, J. C., Cerione, R. A., Mulley, J. C., and Walsh, C. A. (1998) PAK3 mutation in nonsyndromic X-linked mental retardation. *Nat. Genet.* **20,** 25–30
9. Attree, O., Olivos, I. M., Okabe, I., Bailey, L. C., Nelson, D. L., Lewis, R. A., McInnes, R. R., and Nussbaum, R. L. (1992) The Lowe's oculocerebrorenal syndrome gene encodes a protein highly homologous to inositol polyphosphate-5-phosphatase. *Nature* **358,** 239–242
10. Billuart, P., Bienvenu, T., Ronce, N., des Portes, V., Vinet, M. C., Zemni, R., Roest Crollius, H., Carrie, A., Fauchereau, F., Cherry, M., Briault, S., Hamel, B., Fryns, J. P., Beldjord, C., Kahn, A., Moraine, C., and Chelly, J. (1998) Oligophrenin-1 encodes a rhoGAP protein involved in X-linked mental retardation. *Nature* **392,** 923–926
11. Frangiskakis, J. M., Ewart, A. K., Morris, C. A., Mervis, C. B., Bertrand, J., Robinson, B. F., Klein, B. P., Ensing, G. J., Everett, L. A., Green, E. D., Proschel, C., Gutowski, N. J., Noble, M., Atkinson, D. L., Odelberg, S. J., and Keating, M. T. (1996) LIM-kinase1 hemizygosity implicated in impaired visuospatial constructive cognition. *Cell* **86,** 59–69
12. Kutsche, K., Yntema, H., Brandt, A., Jantke, I., Nothwang, H. G., Orth, U., Boavida, M. G., David, D., Chelly, J., Fryns, J. P., Moraine, C., Ropers, H. H., Hamel, B. C., van Bokhoven, H., and Gal, A. (2000) Mutations in ARHGEF6, encoding a guanine nucleotide exchange factor for Rho GTPases, in patients with X-linked mental retardation. *Nat. Genet.* **26,** 247–250
13. Pieretti, M., Zhang, F. P., Fu, Y. H., Warren, S. T., Oostra, B. A., Caskey, C. T., and Nelson, D. L. (1991) Absence of expression of the FMR-1 gene in fragile X syndrome. *Cell* **66,** 817–822
14. Mowrey, P. N., Chorney, M. J., Venditti, C. P., Latif, F., Modi, W. S., Lerman, M. I., Zbar, B., Robins, D. B., Rogan, P. K., and Ladda, R. L. (1993) Clinical and molecular analyses of deletion 3p25-pter syndrome. *Am. J. Med. Genet.* **46,** 623–629
15. Bacon, C., Endris, V., and Rappold, G. (2009) Dynamic expression of the Slit-Robo GTPase activating protein genes during development of the murine nervous system. *J. Comp. Neurol.* **513,** 224–236
16. Waltereit, R., Kautt, S., and Bartsch, D. (2008) Expression of MEGAP mRNA during embryonic development. *Gene Expr. Patterns* **8,** 307–310
17. Endris, V., Wogatzky, B., Leimer, U., Bartsch, D., Zatyka, M., Latif, F., Maher, E. R., Tariverdian, G., Kirsch, S., Karch, D., and Rappold, G. A. (2002) The novel Rho-GTPase activating gene MEGAP/ srGAP3 has a putative role in severe mental retardation. *Proc. Natl. Acad. Sci. U. S. A.* **99,** 11754–11759
18. Soderling, S. H., Binns, K. L., Wayman, G. A., Davee, S. M., Ong, S. H., Pawson, T., and Scott, J. D. (2002) The WRP component of the WAVE-1 complex attenuates Rac-mediated signalling. *Nat. Cell Biol.* **4,** 970–975
19. Yang, Y., Marcello, M., Endris, V., Saffrich, R., Fischer, R., Trendelenburg, M. F., Sprengel, R., and Rappold, G. (2006) MEGAP impedes cell migration via regulating actin and microtubule dynamics and focal complex formation. *Exp. Cell Res.* **312,** 2379–2393
20. Hamdan, F. F., Gauthier, J., Pellerin, S., Dobrzeniecka, S., Marineau, C., Fombonne, E., Mottron, L., Lafreniere, R. G., Drapeau, P., Lacaille, J. C., Rouleau, G. A., and Michaud, J. L. (2009) No association between SRGAP3/MEGAP haploinsufficiency and mental retardation. *Arch. Neurol.* **66,** 675–676
21. Cook, E. H., Jr., and Scherer, S. W. (2008) Copy-number variations associated with neuropsychiatric conditions. *Nature* **455,** 919–923
22. Guilmatre, A., Dubourg, C., Mosca, A. L., Legallic, S., Goldenberg, A., Drouin-Garraud, V., Layet, V., Rosier, A., Briault, S., Bonnet-Brilhault, F., Laumonnier, F., Odent, S., Le Vacon, G., Joly-Helas, G., David, V., Bendavid, C., Pinoit, J. M., Henry, C., Impallomeni, C., Germano, E., Tortorella, G., Di Rosa, G., Barthelemy, C., Andres, C., Faivre, L., Frebourg, T., Saugier Veber, P., and Campion, D. (2009) Recurrent rearrangements in synaptic and neurodevelopmental genes and shared biologic pathways in schizophrenia, autism, and mental retardation. *Arch. Gen. Psychiatry* **66,** 947–956
23. Mitchell, K. J. (2010) The genetics of neurodevelopmental disease. *Curr. Opin. Neurobiol.* **21,** 1–7
24. Morrow, E. M. (2010) Genomic copy number variation in disorders of cognitive development. *J. Am. Acad. Child Adolesc. Psychiatry* **49,** 1091–1104
25. Sebat, J., Levy, D. L., and McCarthy, S. E. (2009) Rare structural variants in schizophrenia: one disorder, multiple mutations; one mutation, multiple disorders. *Trends Genet.* **25,** 528–535
26. Lewis, C. M., Levinson, D. F., Wise, L. H., DeLisi, L. E., Straub, R. E., Hovatta, I., Williams, N. M., Schwab, S. G., Pulver, A. E., Faraone, S. V., Brzustowicz, L. M., Kaufmann, C. A., Garver, D. L., Gurling, H. M., Lindholm, E., Coon, H., Moises, H. W., Byerley, W., Shaw, S. H., Mesen, A., Sherrington, R., O'Neill, F. A., Walsh, D., Kendler, K. S., Ekelund, J., Paunio, T., Lonnqvist, J., Peltonen, L., O'Donovan, M. C., Owen, M. J., Wildenauer, D. B., Maier, W., Nestadt, G., Blouin, J. L., Antonarakis, S. E., Mowry, B. J., Silverman, J. M., Crowe, R. R., Cloninger, C. R., Tsuang, M. T., Malaspina, D., Harkavy-Friedman, J. M., Svrakic, D. M., Bassett, A. S., Holcomb, J., Kalsi, G., McQuillin, A., Brynjolfson, J., Sigmundsson, T., Petursson, H., Jazin, E., Zoega, T., and Helgason, T. (2003) Genome scan meta-analysis of schizophrenia and bipolar disorder. Part II: schizophrenia. *Am. J. Hum. Genet.* **73,** 34–48
27. Addington, A. M., and Rapoport, J. L. (2009) The genetics of childhood-onset schizophrenia: when madness strikes the prepubescent. *Curr. Psychiatry Rep.* **11,** 156–161
28. Stefansson, H., Rujescu, D., Cichon, S., Pietilainen, O. P., Ingason, A., Steinberg, S., Fossdal, R., Sigurdsson, E., Sigmundsson, T., Buizer-Voskamp, J. E., Hansen, T., Jakobsen, K. D., Muglia, P., Francks, C., Matthews, P. M., Gylfason, A., Halldorsson, B. V., Gudbjartsson, D., Thorgeirsson, T. E., Sigurdsson, A., Jonasdottir, A., Jonasdottir, A., Bjornsson, A., Mattiasdottir, S., Blondal, T., Haraldsson, M., Magnusdottir, B. B., Giegling, I., Moller, H. J., Hartmann, A., Shianna, K. V., Ge, D., Need, A. C., Crombie, C., Fraser, G., Walker, N., Lonnqvist, J., Suvisaari, J., Tuulio-Henriksson, A., Paunio, T., Toulopoulou, T., Bramon, E., Di Forti, M., Murray, R., Ruggeri, M., Vassos, E., Tosato, S., Walshe, M., Li, T., Vasilescu, C., Muhleisen, T. W., Wang, A. G., Ullum, H., Djurovic, S., Melle, I., Olesen, J., Kiemeney, L. A., Franke, B., Sabatti, C., Freimer, N. B., Gulcher, J. R., Thorsteinsdottir, U., Kong, A., Andreassen, O. A., Ophoff, R. A., Georgi, A., Rietschel, M., Werge, T., Petursson, H., Goldstein, D. B., Nothen, M. M., Peltonen, L., Collier, D. A., St Clair, D., and Stefansson, K. (2008) Large recurrent microdeletions associated with schizophrenia. *Nature* **455,** 232–236
29. Hayashi-Takagi, A., Takaki, M., Graziane, N., Seshadri, S., Murdoch, H., Dunlop, A. J., Makino, Y., Seshadri, A. J., Ishizuka, K., Srivastava, D. P., Xie, Z., Baraban, J. M., Houslay, M. D., Tomoda, T., Brandon, N. J., Kamiya, A., Yan, Z., Penzes, P., and Sawa, A. (2010) Disrupted-in-schizophrenia 1 (DISC1) regulates spines of the glutamate synapse via Rac1. *Nat. Neurosci.* **13,** 327–332
30. Gailus-Durner, V., Fuchs, H., Becker, L., Bolle, I., Brielmeier, M., Calzada-Wack, J., Elvert, R., Ehrhardt, N., Dalke, C., Franz, T. J., Grundner-Culemann, E., Hammelbacher, S., Holter, S. M., Holzlwimmer, G., Horsch, M., Javaheri, A., Kalaydjiev, S. V., Klempt, M., Kling, E., Kunder, S., Lengger, C., Lisse, T., Mijalski, T., Naton, B., Pedersen, V., Prehn, C., Przemeck, G., Racz, I., Reinhard, C., Reitmeir, P., Schneider, I., Schrewe, A., Steinkamp, R., Zybill, C., Adamski, J., Beckers, J., Behrendt, H., Favor, J., Graw, J., Heldmaier, G., Hofler, H., Ivandic, B., Katus, H., Kirchhof, P., Klingenspor, M., Klopstock, T., Lengeling, A., Muller, W., Ohl, F., Ollert, M., Quintanilla-Martinez, L., Schmidt, J., Schulz, H., Wolf, E., Wurst, W., Zimmer, A., Busch, D. H., and de Angelis, M. H. (2005) Introducing the German Mouse Clinic: open access platform for standardized phenotyping. *Nat. Methods* **2,** 403–404
31. Nagy, A., Rossant, J., Nagy, R., Abramow-Newerly, W., and Roder, J. C. (1993) Derivation of completely cell culture-derived mice from early-passage embryonic stem cells. *Proc. Natl. Acad. Sci. U. S. A.* **90,** 8424–8428
32. Ramon-Moliner, E. (1970) *The Golgi-Cox Technique*, Springer, New York

33. Von Bohlen und Halbach, O., Zacher, C., Gass, P., and Unsicker, K. (2006) Age-related alterations in hippocampal spines and deficiencies in spatial memory in mice. *J. Neurosci. Res.* **83,** 525–531
34. Von Bohlen und Halbach, O., Minichiello, L., and Unsicker, K. (2008) TrkB but not trkC receptors are necessary for postnatal maintenance of hippocampal spines. *Neurobiol. Aging* **29,** 1247–1255
35. Gailus-Durner, V., Fuchs, H., Adler, T., Aguilar Pimentel, A., Becker, L., Bolle, I., Calzada-Wack, J., Dalke, C., Ehrhardt, N., Ferwagner, B., Hans, W., Holter, S. M., Holzlwimmer, G., Horsch, M., Javaheri, A., Kallnik, M., Kling, E., Lengger, C., Morth, C., Mossbrugger, I., Naton, B., Prehn, C., Puk, O., Rathkolb, B., Rozman, J., Schrewe, A., Thiele, F., Adamski, J., Aigner, B., Behrendt, H., Busch, D. H., Favor, J., Graw, J., Heldmaier, G., Ivandic, B., Katus, H., Klingenspor, M., Klopstock, T., Kremmer, E., Ollert, M., Quintanilla-Martinez, L., Schulz, H., Wolf, E., Wurst, W., and de Angelis, M. H. (2009) Systemic first-line phenotyping. *Methods Mol. Biol.* **530,** 463–509
36. Waltereit, R., Welzl, H., Dichgans, J., Lipp, H. P., Schmidt, W. J., and Weller, M. (2006) Enhanced episodic-like memory and kindling epilepsy in a rat model of tuberous sclerosis. *J. Neurochem.* **96,** 407–413
37. Joyner, A. L. (2000) *Gene Targeting: A Practical Approach*, Oxford University Press, Oxford, UK
38. Benard, V., and Bokoch, G. M (2002) Assay of Cdc42, Rac, and Rho GTPase activation by affinity methods. *Methods Enzymol.* **345,** 349–359
39. Mohl, M., Winkler, S., Wieland, T., and Lutz, S (2006) Gef10–the third member of a Rho-specific guanine nucleotide exchange factor subfamily with unusual protein architecture. *Naunyn Schmiedebergs Arch. Pharmacol.*, **373,** 333–341
40. Schneider, I., Tirsch, W. S., Faus-Kessler, T., Becker, L., Kling, E., Busse, R. L., Bender, A., Feddersen, B., Tritschler, J., Fuchs, H., Gailus-Durner, V., Englmeier, K. H., de Angelis, M. H., and Klopstock, T. (2006) Systematic, standardized and comprehensive neurological phenotyping of inbred mice strains in the German Mouse Clinic. *J. Neurosci. Methods* **157,** 82–90
41. Rogers, D. C., Fisher, E. M., Brown, S. D., Peters, J., Hunter, A. J., and Martin, J. E. (1997) Behavioral and functional analysis of mouse phenotype: SHIRPA, a proposed protocol for comprehensive phenotype assessment. *Mamm. Genome* **8,** 711–713
42. Deussing, J. M., Breu, J., Kuhne, C., Kallnik, M., Bunck, M., Glasl, L., Yen, Y. C., Schmidt, M. V., Zurmuhlen, R., Vogl, A. M., Gailus-Durner, V., Fuchs, H., Holter, S. M., Wotjak, C. T., Landgraf, R., de Angelis, M. H., Holsboer, F., and Wurst, W. (2010) Urocortin 3 modulates social discrimination abilities via corticotropin-releasing hormone receptor type 2. *J. Neurosci.* **30,** 9103–9116
43. Schneider, M., Spanagel, R., Zhang, S. J., Bading, H., and Klugmann, M. (2007) Adeno-associated virus (AAV)-mediated suppression of Ca2+/calmodulin kinase IV activity in the nucleus accumbens modulates emotional behaviour in mice. *BMC Neurosci.* **8,** 105
44. Schwartz, M. (2004) Rho signalling at a glance. *J. Cell Sci.* **117,** 5457–5458
45. Schurr, P. H., McLaurin, R. L., and Ingraham, F. D. (1953) Experimental studies on the circulation of the cerebrospinal fluid and methods of producing communicating hydrocephalus in the dog. *J. Neurosurg.* **10,** 515–525
46. Zhang, J., Williams, M. A., and Rigamonti, D. (2006) Genetics of human hydrocephalus. *J. Neurol.* **253,** 1255–1266
47. Steen, R. G., Mull, C., McClure, R., Hamer, R. M., and Lieberman, J. A. (2006) Brain volume in first-episode schizophrenia: systematic review and meta-analysis of magnetic resonance imaging studies. *Br. J. Psychiatry* **188,** 510–518
48. Chen, Y. J., Johnson, M. A., Lieberman, M. D., Goodchild, R. E., Schobel, S., Lewandowski, N., Rosoklija, G., Liu, R. C., Gingrich, J. A., Small, S., Moore, H., Dwork, A. J., Talmage, D. A., and Role, L. W. (2008) Type III neuregulin-1 is required for normal sensorimotor gating, memory-related behaviors, and corticostriatal circuit components. *J. Neurosci.* **28,** 6872–6883
49. Mata, I., Perez-Iglesias, R., Roiz-Santianez, R., Tordesillas-Gutierrez, D., Gonzalez-Mandly, A., Vazquez-Barquero, J. L., and Crespo-Facorro, B. (2009) A neuregulin 1 variant is associated with increased lateral ventricle volume in patients with first-episode schizophrenia. *Biol. Psychiatry* **65,** 535–540
50. Shen, S., Lang, B., Nakamoto, C., Zhang, F., Pu, J., Kuan, S. L., Chatzi, C., He, S., Mackie, I., Brandon, N. J., Marquis, K. L., Day, M., Hurko, O., McCaig, C. D., Riedel, G., and St Clair, D. (2008) Schizophrenia-related neural and behavioral phenotypes in transgenic mice expressing truncated Disc1. *J. Neurosci.* **28,** 10893–10904
51. Chen, L., Liao, G., Waclaw, R. R., Burns, K. A., Linquist, D., Campbell, K., Zheng, Y., and Kuan, C. Y. (2007) Rac1 controls the formation of midline commissures and the competency of tangential migration in ventral telencephalic neurons. *J. Neurosci.* **27,** 3884–3893
52. Kassai, H., Terashima, T., Fukaya, M., Nakao, K., Sakahara, M., Watanabe, M., and Aiba, A. (2008) Rac1 in cortical projection neurons is selectively required for midline crossing of commissural axonal formation. *Eur. J. Neurosci.* **28,** 257–267
53. Blanpied, T. A., and Ehlers, M. D. (2004) Microanatomy of dendritic spines: emerging principles of synaptic pathology in psychiatric and neurological disease. *Biol. Psychiatry* **55,** 1121–1127
54. Halpain, S., Spencer, K., and Graber, S. (2005) Dynamics and pathology of dendritic spines. *Prog. Brain Res.* **147,** 29–37
55. Ramakers, G. J. (2002) Rho proteins, mental retardation and the cellular basis of cognition. *Trends Neurosci.* **25,** 191–199
56. van Spronsen, M., and Hoogenraad, C. C. (2010) Synapse pathology in psychiatric and neurologic disease. *Curr. Neurol. Neurosci. Rep.* **10,** 207–214
57. Calabrese, B., Wilson, M. S., and Halpain, S. (2006) Development and regulation of dendritic spine synapses. *Physiology* **21,** 38–47
58. Penzes, P., Beeser, A., Chernoff, J., Schiller, M. R., Eipper, B. A., Mains, R. E., and Huganir, R. L. (2003) Rapid induction of dendritic spine morphogenesis by trans-synaptic ephrinB-EphB receptor activation of the Rho-GEF kalirin. *Neuron* **37,** 263–274
59. Oh, D., Han, S., Seo, J., Lee, J. R., Choi, J., Groffen, J., Kim, K., Cho, Y. S., Choi, H. S., Shin, H., Woo, J., Won, H., Park, S. K., Kim, S. Y., Jo, J., Whitcomb, D. J., Cho, K., Kim, H., Bae, Y. C., Heisterkamp, N., Choi, S. Y., and Kim, E. (2010) Regulation of synaptic Rac1 activity, long-term potentiation maintenance, and learning and memory by BCR and ABR Rac GTPase-activating proteins. *J. Neurosci.* **30,** 14134–14144
60. Sweatt, J. D. (2003) *Mechanisms of Memory*, Academic Press, San Diego, CA, USA
61. Arguello, P. A., and Gogos, J. A. (2010) Cognition in mouse models of schizophrenia susceptibility genes. *Schizophr. Bull.* **36,** 289–300
62. Nestler, E. J., and Hyman, S. E. (2010) Animal models of neuropsychiatric disorders. *Nat. Neurosci.* **13,** 1161–1169
63. O'Tuathaigh, C. M., Kirby, B. P., Moran, P. M., and Waddington, J. L. (2010) Mutant mouse models: genotype-phenotype relationships to negative symptoms in schizophrenia. *Schizophr. Bull.* **36,** 271–288
64. Van den Buuse, M. (2010) Modeling the positive symptoms of schizophrenia in genetically modified mice: pharmacology and methodology aspects. *Schizophr. Bull.* **36,** 246–270
65. Shprecher, D., and Kurlan, R. (2009) The management of tics. *Mov. Disord.* **24,** 15–24
66. Ko, Y. H., Jung, S. W., Joe, S. H., Lee, C. H., Jung, H. G., Jung, I. K., Kim, S. H., and Lee, M. S. (2007) Association between serum testosterone levels and the severity of negative symptoms in male patients with chronic schizophrenia. *Psychoneuroendocrinology* **32,** 385–391
67. Carlson, B. R., Lloyd, K. E., Kruszewski, A., Kim, I. H., Rodriguiz, R. M., Heindel, C., Faytell, M., Dudek, S. M., Wetsel, W. C., and Soderling, S. H. (2011) WRP/srGAP3 facilitates the initiation of spine development by an inverse F-BAR domain, and its loss impairs long-term memory. *J. Neurosci.* **31,** 2447–2460
68. Shuib, S., McMullan, D., Rattenberry, E., Barber, R. M., Rahman, F., Zatyka, M., Chapman, C., Macdonald, F., Latif, F., Davison, V., and Maher, E. R. (2009) Microarray based analysis of 3p25-p26 deletions (3p- syndrome). *Am. J. Med. Genet. A.* **149A,** 2099–2105

Received for publication April 20, 2012.
Accepted for publication July 10, 2012.